Tyrosine Mediated Tryptophan ATP Sensitivity in Skeletal Myosin†

Sungjo Park and Thomas P. Burghardt*

Department of Biochemistry and Molecular Biology, Mayo Foundation, 200 First Street Southwest, Rochester, Minnesota 55905

Received August 21, 2001; Revised Manuscript Received November 8, 2001

ABSTRACT: Myosin is the molecular motor in muscle that generates torque and transiently reacts with actin. The mechanical work performed by the motor occurs by successive decrements in the free energy of the myosin−nucleotide system. The seat of these transitions is the globular "head" domain of the myosin molecule (subfragment 1 or S1). A very useful (hitherto empirical) signal of these transitions has been optical, namely, detection of state-dependent changes in absorbance or fluorescence of S1. This effect has now been found to arise in a particular myosin residue (Trp510 in rabbit skeletal muscle), enabling the study of its intimate mechanism. In this work, based on measuring time-dependent signals, we find that the signal change upon nucleotide binding is adequately explained by assuming that nucleotide binding to a remote site causes a transition from a situation in which Trp510 is strongly statically quenched to a situation in which it is weakly statically quenched. The Trp510−static quencher interaction is also responsible, in part, for the changing tryptophan optical density in S1 upon nucleotide binding. Using crystallographically based geometry, calculation of the Trp510 electronic wave function indicates that Tyr503 is the static quencher.

Skeletal myosin is a motor protein functioning in muscle as the chemomechanical energy transducer (*2*). As such, this protein, in association with actin and ATP, transduces the chemical free energy in ATP to mechanical work. The globular head of the myosin cross-bridge, separated from its tail to generate subfragment 1 (S1),[1] competently carries out all of the functions of transduction (*3*). For this reason, S1 is thought to contain the necessary elements of the motor except for those residing in the actin (*4*). S1 crystallographic structures suggest it is an articulated molecule made from intact catalytic and lever arm domains that change their relationship during transduction because of a conformation change in the joining converter region (*5*−*10*). The rotating cross-bridge model (*11*, *12*), modified to accommodate crystallographic and mutagenesis data (*13*), simulates contraction by invoking a swinging lever arm while the actin-bound catalytic domain holds a fixed position during force generation. Alternative models assign a more active role to actin (*4*).

ATP hydrolysis occurs in a binding site of the S1 catalytic domain. From there, the effects of hydrolysis influence remote sites, including locations where actin binds and where torque is generated. The influences generated in hydrolysis propagate throughout S1 to the remote sites via pathways that, when known, will shape our models for transduction. Upon ATP binding, S1 tryptophan fluorescence increases for myosins originating from a variety of muscle types (skeletal, smooth, cardiac) and organisms (*14*−*18*). This universal effect places the ATP sensitive tryptophan (AST) in the energy transduction pathway of S1, stimulating interest in locating the responsible residue and the enhancement mechanism (*19*). Early efforts focused on tryptophans near the active site (*20*) and on other tryptophans with side chains susceptible to chemical attack (*21*). We demonstrated some time ago that (in skeletal muscle myosin) Trp510 is an AST but allowed for the possibility that other residues contributed to the total fluorescence increase of S1 upon ATP binding (*22*). Recently, site-directed mutagenesis clarified the issue for two myosins. A mutant of Dictyostelium S1 (DcS1) with tyrosine replacing Trp510 showed no tryptophan fluorescence change upon ATP binding (*16*). Mutants of smooth muscle myosin showed that only Trp510 endows the protein with AST fluorescence (*17*, *18*). These data convincingly demonstrated that, for practical purposes, Trp510 is the sole AST in smooth and DcS1. Lately, we established a similar conclusion for rabbit skeletal S1 (*23*).

The identification of Trp510 as the sole AST allows for the application of a powerful spectroscopic technique on this single residue to elucidate its role in transduction. The Trp510 fluorescence intensity amplitude and lifetime are independently quantifiable by using time-resolved fluorescence measurements. These parameters are inequivalently affected by static and by collisional quenching. Static quenching primarily affects intensity amplitude, while collisional quenching primarily affects lifetime (*24*). By observing the effect of nucleotide binding on the amplitude and lifetime of Trp510 fluorescence decay, we can discover the mechanism imposing ATP sensitivity. Reduced static quenching upon nucleotide binding might indicate the Trp510 indole interacts less strongly with a local side chain or peptide backbone group.

† This work was supported by the National Institutes of Health Grant R01 AR39288 and by the Mayo Foundation.

* Corresponding author. Phone: (507) 284-8120. Fax: (507) 284-9349. E-mail: burghardt@mayo.edu.

[1] Abbreviations: AST, ATP sensitive tryptophan; DcS1, Dictyostelium S1; S1, myosin subfragment 1; SH1, highly reactive thiol or Cys707 in S1; Trp510, ATP sensitive tryptophan; 5′F-S1, 5′IAF modifying SH1 in S1; 5′IAF, 5′-iodoacetamidofluorescein. (Myosin sequence numbering throughout the manuscript is that of chicken pectoralis muscle (*1*).)

10.1021/bi0157058 CCC: $22.00
Published on Web 01/10/2002

Reduced collisional quenching upon nucleotide binding might indicate decreased Trp510 indole interaction with solvent. Candidate static quenching groups are identified by inspecting the available S1 crystal structures.

Knowing the quenching mechanism enables a more accurate interpretation of fluorescence changes and a deeper insight into the conformation changes that accompany transduction. Time-resolved Trp510 fluorescence has elucidated the mechanism of tryptophan ATP sensitivity in a truncated mutant of DcS1 (*25*). The present work investigates the phenomena in rabbit skeletal S1.

MATERIALS AND METHODS

Chemicals. ATP, ADP, dithiothreitol (DTT), TES, *N*-acetyl-L-tryptophanamide (NATA), sodium azide, phenylmethane sulfonyl fluoride (PMSF), and Tris are from Sigma (St. Louis, MO). 5′-Iodoacetamidofluorescein (5′IAF) is from Molecular Probes (Eugene, OR). Acrylamide (ultrapure) was from ICN (Aurora, OH). All other chemicals are reagent grade.

Solutions. Acrylamide stock solution (3 M) was stored in the dark. A stock solution of $BeCl_2$ (88 mM Be, atomic absorption standard solution in 1% HCl) was adjusted to pH 5.0 by the addition of NaOH. Potassium fluoride (KF) stock solution was prepared on the day it was used.

Preparation and Labeling of Myosin S1. Rabbit myosin was prepared from back and leg muscles by the method of Tonomura et al. (*26*). S1 was obtained by digestion of myosin filaments with α-chymotrypsin, as described by Weeds and Taylor (*27*).

5′IAF modification of SH1 (Cys707) in S1 (5′F-S1) was carried out with a 1.4−1.8-fold molar excess of 5′IAF for 18−20 h at 4 °C in the dark, as described previously (*28*). We incorporated 0.70−0.85 5′IAF groups per S1, as inferred from K^+-EDTA and Ca^{2+} ATPase activities (*29*, *30*). Unreacted 5′IAF was normally not removed from the 5′F-S1 samples because its presence did not influence the tryptophan fluorescence observed in our experiments.

Myosin S1 ATPase. ATPase activity of S1 was measured from inorganic phosphate production using the Fiske and Subbarow method (*31*) and was expressed as a percent of control S1. K^+-EDTA ATPase measurements were made on samples at 25 °C from 1 mL aliquots containing 0.26−0.35 μM S1, 2 mM ATP, 0.6 M KCl, 25 mM Tris HCl (pH 8), and 6 mM EDTA. Ca^{2+} ATPase was measured as that for K^+-EDTA ATPase except that 6 mM $CaCl_2$ replaced the 6 mM EDTA.

Preparation of Nucleotide-Bound or Trapped Nucleotide Analogue S1 and 5′F-S1. Myosin S1 or 5′F-S1 was trapped with beryllium or aluminum, as described previously (*32*). When trapped, K^+-EDTA activities for S1 and Ca^{2+} ATPase activities for 5′F-S1 were inhibited by ≥90%. For lifetime experiments in the presence of ATP or ADP, S1 or 5′F-S1 was incubated with 3 mM $MgCl_2$ and 3 mM ATP or 1 mM $MgCl_2$ and 0.25 mM ADP. For absorption experiments in the presence of ATP or ADP, S1 was incubated with 1 mM $MgCl_2$ and 1 mM ATP or 1 mM $MgCl_2$ and 0.25 mM ADP.

Nucleotide Analogue Induced Structures of S1. The principal chemical states during S1 ATPase are collected in Scheme 1where M, M*, M**, and M^ represent distinct myosin conformations. The steady-state fractional concentrations of the intermediates are known for a variety of myosins (*15*, *33*−*35*), all having M**·ADP·P_i as the predominant intermediate (*36*).

Scheme 1

$$M+ATP \leftrightarrow M^*.ATP \leftrightarrow M^{**}.ADP.Pi \leftrightarrow M\hat{}.ADP + Pi \leftrightarrow M+ADP$$

Facilitating the structural characterization of the transients in Scheme 1 are nucleotide analogues. They reversibly trap the myosin active site and induce structures that statically mimic the transient intermediates in solution. Exhaustive comparison of analogue-induced and transient S1 structures leads to the identification of bound ATPγS (*37*) or trapped ADP·BeF_x (low ionic strength) (*38*) with M*·ATP, trapped ADP·V_i, ADP·AlF_4^-, or ADP·BeF_x (high ionic strength) with M**·ADP·P_i, and bound ADP with M^·ADP (*6*, *39*−*41*). Often, for reasons related to the disposition of the active site, M, M*, and M^ are referred to collectively as "open" conformations, while M** is referred to as a "closed" conformation (*42*).

Time-Resolved Fluorescence Measurements. Tryptophan fluorescence intensity decay was measured on a time-domain analogue lifetime instrument with flash lamp excitation (PTI, London, Ontario, Canada). Tryptophans were excited at 298 nm, and emission was collected over a 32 nm bandwidth centered at 335 nm. All protein measurements were made on 1.2 μM S1 in 0.2 mM DTT and 25 mM TES (pH 7.0) at 7 or 20 °C. Data collection intervals were 30−40 min on protein samples that had identical ATPases before and after the lifetime measurements. We verified instrument calibration using NATA in 0.1 M sodium phosphate (pH 7) and 20 °C having a 3 ns lifetime and quinine bisulfate in 0.1 N H_2SO_4 at 23 °C having an 18.9 ns lifetime. These standards gave 2.95 ± 0.3 and 19.4 ± 0.2 ns, respectively. We verified the ability of the instrument to resolve multiple tryptophan fluorescence lifetimes by analyzing the total tryptophan fluorescence intensity decay of S1. From S1, we obtained three lifetimes of 0.5 ± 0.2, 3.7 ± 0.1, and 8.6 ± 0.4 ns, in good agreement with previous measurements (*43*).

Time-resolved fluorescence intensities were fitted by convoluting the observed lamp profile with an exponential fitting function of the form

$$F(t) = \sum_{i=1}^{p} A_i e^{-t/\tau_i} \quad (1)$$

where A_i is the decay amplitude and τ_i the lifetime for the *i*th component (*44*). Best fits were located using a nonlinear least squares protocol. In all cases, we found Trp510 fluorescence decay was adequately approximated by a single term ($p = 1$) in the sum of eq 1.

Flash lamp light excitation and collected emission polarization can affect the apparent lifetime of samples undergoing rotational diffusion on a timescale comparable with the fluorescence lifetime. Sample rotational relaxation effects are removed from emission decay kinetics by exciting with light that produces emission propagating into the collection optics that is randomly polarized in the plane perpendicular to the direction of propagation. This is accomplished in the PTI instrument, where excitation and emission optics make a 90° angle by polarizing the excitation light parallel or antiparallel to the propagation direction of the collected emitted light. We performed experiments with and without the excitation

polarizer and found no systematic difference in the observed lifetime of Trp510, suggesting rotational relaxation makes no significant contribution. Results shown here originate from measurements without a polarizer because of their better signal-to-noise characteristics.

The isolation of Trp510 emission is accomplished by using 5′IAF to modify, specifically, SH1 in S1 to form 5′F-S1 (*28*). In 5′F-S1, the probe completely quenches Trp510 fluorescence but is too distant from other tryptophans in S1 to affect their fluorescence. Modification of SH1, in and of itself, does not alter tryptophan emission in S1, and these observations hold whether a nucleotide or nucleotide analogue occupies the S1 active site. Under these circumstances, the difference of intensities

$$\Delta I(N) \equiv I(\mathrm{S1}\cdot N) - I(\mathrm{5'F\text{-}S1}\cdot N) \qquad (2)$$

originates solely from Trp510 (*22*, *45*, *46*). *N* in the arguments represents a nucleotide, nucleotide analogue, or when missing, the absence of nucleotide.

We also showed, previously, that the ratio of fluorescence increments due to nucleotide binding, $\{I(\mathrm{5'F\text{-}S1}\cdot N) - I(\mathrm{5'F\text{-}S1})\}/\{I(\mathrm{S1}\cdot N) - I(\mathrm{S1})\}$, decreases linearly with increasing number of SH1 groups modified and extrapolates to zero for 100% 5′IAF modification of SH1. The latter data indicates that Trp510 is the sole AST because no nucleotide fluorescence enhancement occurs in residues other than Trp510 (*23*). Equation 2 holds at every instant in time during the fluorescence decay of tryptophans in S1 or 5′F-S1 so that $\Delta I(N,t)$ is the time-dependence of the Trp510 fluorescence decay in the presence of *N*.

Stern−Volmer constants for acrylamide quenching of Trp510 were estimated from the Trp510 lifetime using the relation

$$\frac{\tau_0}{\tau} = 1 + K_{\mathrm{SV}}[\mathrm{C}] \qquad (3)$$

where [C] is acrylamide concentration and τ_0 is the Trp510 lifetime in the absence of acrylamide (*47*). Acrylamide quenching data, wherein τ_0/τ is plotted as a function of quencher concentration for $0 \le [\mathrm{C}] \le 0.15$ M using eq 3, were fitted with a line whose slope is the free parameter K_{SV}.

Absorption Spectroscopy. Absorption spectra were measured on a Cary 4E absorption spectrophotometer (Varian, Mulgrave Victoria, Australia). All measurements were made in a tandem absorption cell on 10−16 μM S1 in 25 mM TES pH 7 at 20 °C.

The difference extinction coefficient spectrum is

$$\Delta\epsilon(N) \equiv \epsilon(\mathrm{S1}\cdot N) - \epsilon(\mathrm{S1}) - \epsilon(N) \qquad (4)$$

where argument *N* usage is identical to that in eq 2, but note that in the absence of nucleotide $\Delta\epsilon(-) = 0$. The spectrum from separated S1 and *N* samples was subtracted from the S1·*N* spectrum observed when the same two components were mixed. At wavelengths $\gtrsim$298 nm, $\Delta\epsilon(N)$ is from the enhancement of Trp510 extinction due to the binding of *N*.

Trp510 Fluorescence Quenching Mechanism. A model for Trp510 quenching in S1 has a quenching group Q within S1 changing its relationship with the Trp510 indole as S1 assumes the transient conformations occurring during ATPase. Scheme 2 represents the quenching mechanism for a particular S1 conformation with chemical or radiative reactions occurring in the left−right or down−up dimensions. Trp510 existing in ground and excited singlet states, W and W* respectively, interacts with Q similarly existing in a singlet state (*24*). Complex W·Q is sometimes represented by E, anticipating that the excited complex, or exiplex (W·Q)*, is represented by E*. J_0 is the incident photon flux in photons/sec, and $J_0(1 - \exp[-\gamma A_{\mathrm{E}}])$ or $J_0(1 - \exp[-\gamma A_{\mathrm{W}}])$ for $\gamma = \ln(10)$ gives the photostationary light absorption rates for the E or W species from absorption coefficients A_{E} and A_{W}. $K_{\mathrm{S}} = [\mathrm{E}]_{\mathrm{eq}}/[\mathrm{W}]_{\mathrm{eq}}[\mathrm{Q}]_{\mathrm{eq}}$, where $[]_{\mathrm{eq}}$ denotes concentration at equilibrium, is the equilibrium constant for complex formation in the ground state. The constant k_{W} is the relaxation rate for W* in the absence of Q, and k_{E} is the relaxation rate for E* → E. Exiplex E* dissociates to produce W* + Q with rate $k_{\mathrm{W}\leftarrow\mathrm{E}}$. Dynamic quenching occurs with rate $k_{\mathrm{E}\leftarrow\mathrm{W}}[\mathrm{Q}]$.

Scheme 2

$$\begin{array}{ccc} \mathrm{W^*} + \mathrm{Q} & \underset{k_{\mathrm{W}\leftarrow\mathrm{E}}}{\overset{k_{\mathrm{E}\leftarrow\mathrm{W}}}{\rightleftharpoons}} & (\mathrm{W.Q})^* \\ J_0(1-10^{-A_{\mathrm{W}}}) \downarrow\uparrow k_{\mathrm{W}} & & k_{\mathrm{E}} \downarrow\uparrow J_0(1-10^{-A_{\mathrm{E}}}) \\ \mathrm{W} + \mathrm{Q} & \underset{K_s}{\rightleftharpoons} & (\mathrm{W.Q}) \end{array}$$

Matrix form coupled rate equations corresponding to Scheme 2 for time-resolved fluorescence decay are

$$\begin{pmatrix}[\mathrm{W^*}]\\ [\mathrm{E^*}]\end{pmatrix}' = \begin{pmatrix} -k_{\mathrm{W}} - k_{\mathrm{E}\leftarrow\mathrm{W}}\dfrac{\alpha}{K_{\mathrm{S}}(1-\alpha)} & k_{\mathrm{W}\leftarrow\mathrm{E}} \\ k_{\mathrm{E}\leftarrow\mathrm{W}}\dfrac{\alpha}{K_{\mathrm{S}}(1-\alpha)} & -k_{\mathrm{W}\leftarrow\mathrm{E}} - k_{\mathrm{E}} \end{pmatrix}\begin{pmatrix}[\mathrm{W^*}]\\ [\mathrm{E^*}]\end{pmatrix} \equiv B\begin{pmatrix}[\mathrm{W^*}]\\ [\mathrm{E^*}]\end{pmatrix} \qquad (5)$$

where we replaced [Q] with its value in equilibrium (neglecting the exceedingly low excited-state concentrations) $\alpha/K_{\mathrm{S}}(1-\alpha)$ for $\alpha = [\mathrm{E}]_{\mathrm{eq}}/[\mathrm{W}]_{\mathrm{T}}$, $1 - \alpha = [\mathrm{W}]_{\mathrm{eq}}/[\mathrm{W}]_{\mathrm{T}}$, and $[\mathrm{W}]_{\mathrm{T}} = [\mathrm{W}] + [\mathrm{E}]$. $[\mathrm{W}]_{\mathrm{T}}$ is the total concentration of Trp510, neglecting excited-state concentrations. Equations 5 have initial conditions $[\mathrm{W^*}](0) = \kappa J_0\gamma[\mathrm{W}]_{\mathrm{T}}/\epsilon_{\mathrm{W}}(1 - \alpha)$ and $[\mathrm{E^*}](0) = \alpha[\mathrm{W^*}](0)/(1 - \alpha)$ for κJ_0 photons absorbed, $A_{\mathrm{W}} = \epsilon_{\mathrm{W}}\ell$, $A_{\mathrm{E}} = \epsilon_{\mathrm{E}}\ell$, and ℓ the path length. When defined

$$J'_0 \equiv \kappa J_0\gamma[\mathrm{W}]_{\mathrm{T}}\ell, \quad \Omega \equiv B_{1,1} + B_{2,2}, \quad \Delta \equiv B_{1,1} - B_{2,2}, \quad \lambda \equiv \sqrt{(4B_{1,2}B_{2,1} + \Delta^2)} \qquad (6)$$

eqs 5 give the fluorescence intensity from Trp510

$$\frac{\Delta I(t)}{k_{\mathrm{FW}}} = [\mathrm{W^*}](t) = J'_0 e^{-1/2(\Omega+\lambda)t}\left\{\epsilon_{\mathrm{W}}(1-\alpha)\left(\frac{1}{2}\{1 + e^{-\lambda t}\} + \frac{\Delta}{2\lambda}\{1 - e^{-\lambda t}\}\right) + \epsilon_{\mathrm{E}}\alpha\frac{k_{\mathrm{W}\leftarrow\mathrm{E}}}{\lambda}(1 - e^{-\lambda t})\right\} \qquad (7)$$

where k_{FW} is the intrinsic fluorescence decay rate for tryptophan. Equation 7 shows that the biexponential fluo-

rescence decay contains contributions from prompt and delayed processes. Prompt fluorescence has a relative amplitude $\epsilon_W(1 - \alpha)$ and decays in time monotonically from its initial value. Delayed fluorescence, from the repopulation of [W*] by exiplex dissociation, increases from an initial value of zero, reaches a maximum at $t_M = \ln[(\Omega - \lambda)/(\Omega + \lambda)]/\lambda$, then decays with an asymptotic rate equal to that from prompt fluorescence. Delayed fluorescence has a direct contribution with relative amplitude $\epsilon_E\alpha k_{W\leftarrow E}/\lambda$ from absorption by E and an indirect contribution with relative amplitude $\epsilon_W(1 - \alpha)\Delta/2\lambda$ from absorption by W, conversion to an exiplex by collisional quenching, and then reconversion to [W*] by exiplex dissociation. Qualitatively, delayed fluorescence slows fluorescence relaxation or equivalently increases the apparent lifetime of W*.

Two absolute quantities that are readily observable are the relative change in fluorescence decay amplitude, *A*, and relaxation time, Γ, upon nucleotide binding or trapping. The former, by inspection of eq 7,

$$\frac{A(\mathrm{S1}\cdot N)}{A(\mathrm{S1})} = \frac{1 - \alpha(\mathrm{S1}\cdot N)}{1 - \alpha(\mathrm{S1})} \tag{8}$$

shows that an amplitude enhancement in the presence of *N* requires $\alpha(\mathrm{S1}) > \alpha(\mathrm{S1}\cdot N)$ (i.e., a decrease in [E] and an increase in [W] upon nucleotide binding). The relative relaxation times $\Gamma(\mathrm{S1}\cdot N)/\Gamma(\mathrm{S1})$ are more complicated but readily formulated qualitatively by inquiring from eq 7 at what time Γ following $t = 0$ does the Trp510 intensity fall to $1/e \times \Delta I(0)$. The neglect of the second-order delayed fluorescence contribution and assuming $1 \pm e^{-\lambda\Gamma} \approx 1$ gives

$$\frac{\Gamma(\mathrm{S1}\cdot N)}{\Gamma(\mathrm{S1})} = \frac{1 + \ln\left[\frac{1}{2} + \frac{k_{W\leftarrow E}}{\lambda}\frac{\epsilon_E}{\epsilon_W}\frac{\alpha(\mathrm{S1}\cdot N)}{1 - \alpha(\mathrm{S1}\cdot N)}\right]}{1 + \ln\left[\frac{1}{2} + \frac{k_{W\leftarrow E}}{\lambda}\frac{\epsilon_E}{\epsilon_W}\frac{\alpha(\mathrm{S1})}{1 - \alpha(\mathrm{S1})}\right]} \tag{9}$$

Equation 9 indicates that if $\alpha(\mathrm{S1}) > \alpha(\mathrm{S1}\cdot N)$, a shorter relaxation time must be observed in the presence of nucleotide. This result is reasonable because delayed fluorescence contributes more significantly in a sample with larger α (or [E]). Here, we equate τ from eq 1 with Γ from eq 9 because just a single exponential characterizes the time-dependence of the observed fluorescence intensity decay curves.

Optical Signal Calculation. The peak absorption energy and dipole strength for electronic transitions contributing to the near UV absorption of Trp510 in S1 were calculated by the matrix method (*48*), as described previously (*49*). The calculation combines the two observable lowest energy transitions of the peptide amide group, the (n,π^*) and (π,π^*) transitions, with the observable (π,π^*) transitions from aromatic side chains. The Coulomb potential with vacuum dielectric constant couples the transition monopoles of these excited states from interacting groups. The aromatic side chains considered include tryptophan, tyrosine, phenylalanine, and histidine.

The matrix method provides the electronic wave function, $|\mathrm{Trp510}>_i$, for the residues in the neighborhood of Trp510 in ground or excited state *i*. This wave function is constructed from the unperturbed wave functions for noninteracting residues, ϕ_j, such that

$$|\mathrm{Trp510}>_i = \sum_{j=1}^{G} a_{i,j}\varphi_j \tag{10}$$

where $a_{i,j}$ is the coupling coefficient and *G* is the total number of contributing unperturbed wave functions. The $a_{i,j}$'s are orthonormal such that $\sum_{j=1}^{G} a_{i,j}a^*_{i',j} = \delta_{i,i'}$ for $\delta_{i,i'}$, the Kronecker delta.

The unperturbed wave functions are identified with a specific group and electronic transition, for instance Trp510/^{1}L$_a$ and Tyr503/^{1}L$_b$, while $|\mathrm{Trp510}>_i$, is in general delocalized. However, the two lowest energy excited states corresponding to $i = 1$ and 2 are localized to the Trp510/^{1}L$_b$′ and Trp510/^{1}L$_a$′ group/transition, where the prime designates perturbed. This is because their unperturbed counterparts Trp510/^{1}L$_b$ and Trp510/^{1}L$_a$ are the largest contributors to the total wave function and have peak transition energies well separated from those of all other interacting groups. It also turns out that the perturbations to Trp510/^{1}L$_b$ and Trp510/^{1}L$_a$ in S1 are small, making their identification within the total wave function trivial. Subsequently, we will be interested in absorption by Trp510/^{1}L$_a$′.

The coupling coefficient amplitude $(a_{2,j}a^*_{2,j})^{1/2} = |<\phi_j|\mathrm{Trp510}>_2|$ is the electronic coupling strength between the *j*th unperturbed wave function and $|\mathrm{Trp510}>_2$. It is a measure of the contribution of the *j*th group/transition to the total wave function. We are interested in the group or groups (other than Trp510) that most strongly couple to Trp510/^{1}L$_a$′ to discover those responsible for static quenching and absorption enhancement in Trp510. We estimate group coupling strength, *S(k)*, by summing over the *g(k)* transitions attributed to group *k* such that

$$S(k) = \sqrt{\sum_{j=1}^{g(k)} a_{2,j}a^*_{2,j}} \tag{11}$$

When Tyr503 is the group coupling to Trp510/^{1}L$_a$′, *k* corresponds to Tyr503, and the sum over *j* includes the four observable transitions from the phenolic side chain and the two observable lowest energy transitions of the peptide amide group.

Dynamics in the Trp510 and other interacting residue side chains affect the optical signals observed from S1. These movements are slow on the timescale of light absorption and are modeled by static averaging over an ensemble of structures constructed using molecular mechanics. Here, we allow side chain movement in Trp510 and one other nearby interacting residue, consistent with certain constraints, while all other atoms in the S1 structure remain fixed in their crystal structure position. Conformational energy constrains side chain dynamics such that structures exceeding a chosen cutoff energy are excluded from the ensemble. All structures in the ensemble are equally weighted. Conformational energies were computed for a protein system consisting of all residues within 20 Å of Trp510 C_γ with molecular mechanics and the mm+ force field implemented in HyperChem (Hypercube, Gainesville, FL). The inclusion of residues beyond 20 Å had no significant impact on conformational energy.

Table 1: Absorption and Time-Resolved Fluorescence Characterization of Trp510 in Skeletal S1[a]

nucleotide or analogue (*N*)	conformation (Scheme 1)	$\Delta\epsilon$ (M cm)$^{-1}$	lifetime (τ, ns)	amplitude (*A*, arb units)	K_{SV} (M^{-1})
	M		9.4 ± 0.2 (5)	1.00 ± 0.03 (5)	8.6 ± 0.2 (2)
ADP	M^	120 ± 43 (10)	9.2 ± 0.2 (4)	1.06 ± 0.03 (4)	9.1 (1)
ADP·BeF_x	M*	839 ± 93 (7)	8.0 ± 0.2 (2)	1.72 ± 0.19 (2)	7.4 ± 0.4 (2)
ATP	M**	918 ± 90 (10)	7.2 ± 0.3 (4)	2.00 ± 0.17 (4)	6.4 ± 0.1 (3)
ADP·AlF_4^-	M**	1546 ± 42 (4)	7.0 ± 0.3 (3)	2.14 ± 0.25 (3)	5.7 ± 0.2 (2)

[a] Errors indicate standard error of the mean for (*n*) independent measurements. $\Delta\epsilon$, defined in eq 4, is measured at 298 nm. At 298 nm, ϵ(S1) = 10.5×10^3 (M cm)$^{-1}$. Morita estimated ΔOD defined as in eq 4 from heavy meromyosin (HMM) in 80 mM KCl, 10.6 mM $MgCl_2$, 71 μM ATP, and 70 mM Tris HCl (pH 8.0) (*50*). From that data and for S1, we estimate $\Delta\epsilon$(ATP) $\approx$ 1400 (M cm)$^{-1}$, in qualitative agreement with our observations. Lifetimes and amplitudes are defined in eq 1. The K_{SV}'s shown here and determined using eq 3 are for practical purposes identical to those observed previously with steady-state fluorescence (*23*).

RESULTS

Trp510 Nucleotide-Induced Absorption Enhancement. Table 1 summarizes $\Delta\epsilon$ values observed for bound nucleotide or trapped nucleotide analogues at 298 nm excitation. Values are in agreement with previous observations (*50*) and indicate an absorption enhancement of ~1000−1500 (M cm)$^{-1}$ in the M** conformation. This corresponds to a relative absorption enhancement, $\Delta\epsilon$(ATP or ADP·AlF_4^-)/ϵ(S1) of 0.087−0.147. When each tryptophan in S1 is assumed to have the same absorption in the absence of nucleotide, ϵ(S1) = 5ϵ_{510}(S1), where ϵ_{510}(S1) is the extinction coefficient for Trp510 in the absence of nucleotide. Furthermore, $\Delta\epsilon(N) = \epsilon_{510}$(S1·*N*) − ϵ_{510}(S1) so that the Trp510 relative absorption enhancement ϵ_{510}(S1·ATP or S1·ADP·AlF_4^-)/ϵ_{510}(S1) = 1.44−1.74. These data suggest an increase in the Trp510 transition dipole moment, or a red shift in its peak energy (because the absorption peak lies to the blue side of the observed wavelength), upon the formation of the M** conformation. Consideration of the absorption spectral shape from the tryptophan ^1L_b and ^1L_a dipole moments indicates that light absorption at wavelengths $\gtrsim$298 nm is due exclusively to the ^1L_a moment (*51*). Consequently, the observed changes pertain to ^1L_a.

Trp510 Time-Resolved Fluorescence Intensity Decay. Figure 1 shows $\Delta I(N,t)$ computed from eq 2 for S1·ADP·AlF_4^- and S1 without nucleotide. A single exponential fitting function in the form of eq 1 provides an amplitude (*A*) and lifetime (τ) for the Trp510 fluorescence decay. Residuals and their autocorrelation, shown only for the less intense curve, indicate that the data is well approximated by the single exponential function. Trial fitting functions made from the linear combination of two or more exponentials did not improve the χ^2 of the fit.

Table 1 summarizes the Trp510 fluorescence intensity amplitude and lifetime computed from eq 2 for S1 and S1 with bound nucleotide or trapped nucleotide analogues. Also indicated are the Trp510 Stern−Volmer quenching constants (K_{SV}) measured independently using eq 3 and the collisional quencher acrylamide. The K_{SV}'s are smallest for S1's assuming the closed conformation and largest for those assuming the open conformations, indicating that Trp510 is least and most solvent accessible in closed and open conformations, respectively. The K_{SV}'s are independent of how the nucleotide or nucleotide analogue binding to S1 affects Trp510 emission lifetime or amplitude. The Trp510 lifetime decreases when S1 assumes more closed conformations upon nucleotide or nucleotide analogue binding. Because enhanced exposure of Trp510 to a Stern−Volmer quencher diminishes fluorescence lifetime and steady-state intensity, enhanced exposure of Trp510 to any solvent-borne tryptophan quenchers cannot cause the steady-state fluorescence enhancement of Trp510 upon nucleotide binding. Accordingly, an alternative explanation is proposed in Scheme 2 (i.e., that there is a Trp510 quencher Q that is a residue in S1).

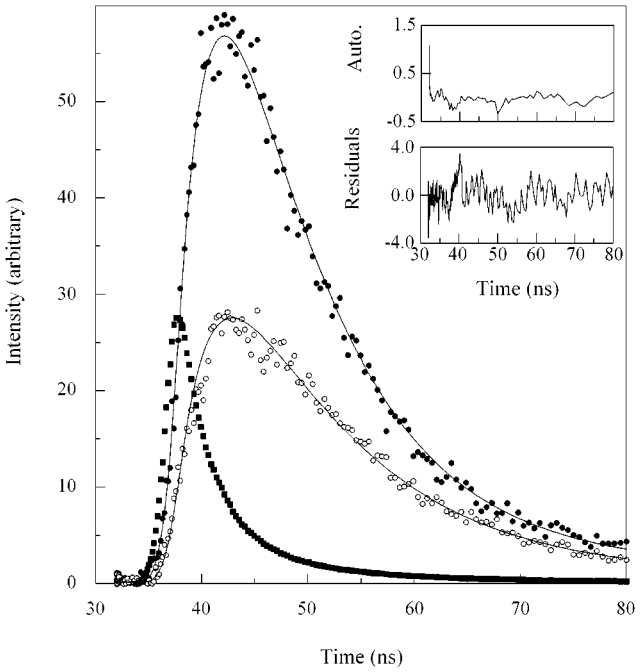

FIGURE 1: Trp510 time-resolved fluorescence intensity from (○) S1 and (●) S1·ADP·AlF_4^- following flash lamp excitation (■). The solid lines are best theoretical fits derived from single exponential fitting functions, as described in Materials and Methods. The residuals shown are the difference between the data and the best fitting theoretical curve for the S1 sample. Similar residuals were obtained for the S1·ADP·AlF_4^- sample. Autocorrelation of the residuals (Auto), amplifying systematic deviations between data and fit, shows that deviations are random. The rapid convergence of the curves over time show the signature effects of bound nucleotide on Trp510 fluorescence (i.e., larger amplitude and shorter lifetime).

The comparison of the decay amplitudes (using eq 8 and the data in Table 1) of M** and M indicates that $[1 - \alpha(M^{**})]/[1 - \alpha(M)] = 2.1 \pm 0.3$. By definition, $0 \leq \alpha \leq 1$ for any α, allowing for the conclusions that $\alpha(M) > \alpha(M^{**})$ and $\alpha(M) \geq 0.52 \pm 0.07$. Thus, we find that more that half of the Trp510s in S1 without nucleotide are in a ground-state complex with the quencher residue referred to as Q in Scheme 2. Then, it follows from eq 9 that the Trp510 fluorescence relaxation time in the M** conformation must

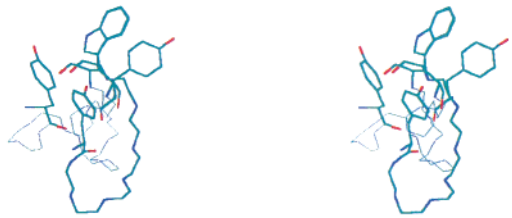

FIGURE 2: Uncrossed stereoview of Tyr503, Trp510, and the joining peptide backbone from skeletal (*5*), smooth (*9*), and scallop myosin S1 (*10*). The skeletal S1 without nucleotide (bolded), smooth muscle S1·ADP·AlF_4^- (only Tyr503 bolded and on the right of Trp510), and scallop muscle S1·ADP (only Tyr503 bolded and on the left of Trp510) structures are shown. Trp510 side chains from the three structures are overlaid. Side chains from the skeletal muscle Tyr503 and Trp510 form an L-shaped conformation, while in smooth and scallop muscle they form a structure more akin to stacked rings.

be shorter than that in the absence of nucleotide. The latter result is consistent with the data reported in Table 1.

*Structural Characterization of Trp510 in M, M^, and M** Conformations*. The nearest aromatic group to Trp510 in the skeletal (M), smooth (M**), or scallop (M^) muscle S1 crystal structures is Tyr503 (*5*, *9*, *10*). Figure 2 shows the relationship of these residues for a fixed Trp510, as the protein assumes the conformations in the crystal structures. In M^ and M**, the Tyr503−Trp510 side chains are approximately "stacked" in contrast to the more "L-shaped" conformation in M.

The peak energy and dipole strength computed for Trp510/$^1L_a'$ in the M, M^, and M** structures are sensitive to the proximity and relative orientation of the Tyr503 side chain. We find that Tyr503 has the largest single residue electronic coupling strength to Trp510/$^1L_a'$ in the M, M^, and M** crystal structures and that, of these structures, the coupling is largest in M. These statements are based on the Trp510 and Tyr503 side chains maintaining their exact conformation in the crystal structures. A more realistic calculation involves side chain dynamics. Kinetic energy and the protein matrix constrain side chain dynamical movement and indirectly influence the observed optical signals. We introduced side chain dynamics to our system by creating an ensemble of structures in which the Trp510 and Tyr503 side chain torsion angles Ω_1 (from atoms N−C_α−C_β−C_γ) and Ω_2 (from atoms C_α−C_β−C_γ−C_δ) vary in a manner consistent with residue conformational energies $\leq E_0 + 5$ kcal/mol, where E_0 is the conformational energy for the residues in the crystal structure. The 5 kcal/mol is the expected energy fluctuation amplitude for the two residues at room temperature. Ensemble averaged coupling strengths and optical signals are summarized in Table 2.

Table 2 shows the ensemble averaged coupling strength, Trp510 dipole strength and relative absorption enhancement, and relative peak absorption energy red shift for the M, M^, and M** conformations. The ensemble averages also show that Tyr503 has the largest single residue electronic coupling strength to Trp510/$^1L_a'$ in the M, M^, and M** crystal structures and that, of these structures, Tyr503-Trp510/$^1L_a'$ coupling is largest in M. This observation agrees with the implications from the fluorescence decay amplitudes where we deduced $\alpha(M) > \alpha(M^{**})$ for α representing the fractional concentration of the (W·Q) complex in Scheme 2. In Table 2, Trp510 absorption is enhanced by the binding of nucleotide in agreement with observation; however, the magnitude of the enhancement is significantly less than that suggested by observation. Computed peak absorption energy is blue shifted by nucleotide binding, suggesting that the observed absorption enhancement is due to changes in the absorption dipole strength rather than to shifts in the peak transition energy.

Nucleotide sensitivity in Trp510 appears to be influenced by the interaction between Trp510 and Tyr503. We replaced selected residues in the S1 crystal structures and recomputed the Trp510 characteristics to clearly identify the residues and interactions responsible for imparting nucleotide sensitivity to Trp510. Replacements investigated were the singly substituted proteins Tyr503Phe or Tyr503Leu and the doubly substituted protein Tyr503Leu and Phe711Leu. When Phe

Table 2: Ensemble Averaged Calculated Properties of the $|Trp510>_2$ Wave function[a]

conformation (Scheme 1)	largest coupling strength (group)[b]	D_{510} (debye^2)[c]	$\frac{\epsilon_{510}(S1\cdot N)}{\epsilon_{510}(S1)}$	red shift (nm)
M (native)	0.090 ± 0.001 (Y503)	4.619 ± 0.009	1	0
M^ (native)	0.023 ± 0.001 (Y503)	4.932 ± 0.019	1.067 ± 0.006	−0.188 ± 0.004
M** (native)	0.031 ± 0.001 (Y503)	4.889 ± 0.012	1.059 ± 0.004	−0.147 ± 0.003
M (Y503F)	0.023 ± 0.002 (F503)	4.921 ± 0.007	1	0
M^ (Y503F)	0.023 ± 0.001 (F503)	5.033 ± 0.005	1.023 ± 0.002	−0.052 ± 0.001
M** (Y503F)	0.017 ± 0.001 (F503)	5.160 ± 0.009	1.049 ± 0.006	−0.044 ± 0.001
M (Y503L)	0.015 ± 0.001 (F711)	5.129 ± 0.022	1	0
M^ (Y503L)	<0.01 (F711)	5.081 ± 0.006	0.991 ± 0.006	+0.007 ± 0.001
M** (Y503L)	0.015 ± 0.001 (F711)	5.356 ± 0.038	1.044 ± 0.012	−0.014 ± 0.001
M (Y503L, F711L)	0.015 ± 0.001 (F512)	5.325 ± 0.019	1	0
M^ (Y503L, F711L)	<0.01 (mixed)	5.087 ± 0.008	0.955 ± 0.005	+0.039 ± 0.003
M** (Y503L, F711L)	<0.01 (F512)	5.145 ± 0.028	0.966 ± 0.009	−0.015 ± 0.001

[a] Errors indicate standard error of the mean, with the number of samples in the ensemble ranging from 12 to 315. Mutations investigated include Tyr503Phe, Tyr503Leu, and Phe711Leu, as noted under the "conformation" heading. [b] Ensemble averaged coupling strength between $|Trp510>_2$ and the unperturbed wave functions of the group in parentheses computed with eq 11. The coupling strength listed is the largest value for any single group in a given structure. [c] Dipole strength, D_{510}, is proportional to the extinction coefficient and given by the relationship,

$$D_j = |<0|\vec{\mu}|Trp510>_2|^2 = 9.18 \times 10^{-3} \int \frac{n\epsilon_j(\lambda)}{\lambda\beta^2}\, d\lambda$$

where $\vec{\mu}$ is the dipole moment operator, λ is wavelength, and $\beta = (n^2 + 2)/3$ for the protein imbedded in a medium of refractive index n. The appropriate ratio of dipole strengths is the relative Trp510 absorption enhancements given in the next column.

replaced Tyr, the benzoic replaced the phenolic ring. When Leu replaced Tyr or Phe, the C_δ's of the leucine side chain were placed at or near the C_δ's of the aromatic ring of Tyr or Phe, and then the leucine side chain atoms were allowed to move to find an optimized geometry while all other atoms in the protein remained fixed. Leucine rotamers do not influence computed coupling strengths or optical signals of aromatic residues; hence, the dynamics of these atoms was not represented in the ensemble of structures. The ensemble averaged quantities computed from S1 mutants are summarized in Table 2.

Table 2 results show that the single substitutions Tyr503Phe or Tyr503Leu eliminate strong coupling of Trp510/$^1L_a'$ to any preferred group. As the coupling strength is a measure of the overlap of the electronic wave functions, a requirement for static quenching, either the Tyr503Phe or the Tyr503Leu substitution should greatly attenuate the nucleotide sensitivity of Trp510 fluorescence. In Tyr503Phe or Tyr503Leu substituted S1, the Phe503 or Phe711 side chains groups are the predominant couplers to Trp510/$^1L_a'$, although the coupling strength is weak. We find that Tyr503 has the same role in each of the S1 conformations (i.e., to reduce the absorption dipole moment of Trp510) because the replacement of Tyr503 with phenylalanine or leucine uniformly causes an increase in the dipole moment of Trp510 (compare values for dipole strength). The Tyr503Phe substitution slightly attenuates the nucleotide sensitivity of Trp510 absorption. The Tyr503Leu substitution removes or attenuates the nucleotide sensitivity of Trp510 absorption in scallop or smooth muscle myosin. Substitutions of Tyr503Leu and Phe711Leu together completely remove the nucleotide sensitivity of Trp510 absorption (compare values for the ratio of extinction coefficients).

DISCUSSION

With reasonable assurance that the ATP sensitive tryptophan is Trp510 (*16*−*18*, *23*), we seek to elucidate the molecular mechanism of its ATP sensitivity. The investigation is motivated by the apparent connection between ATP-induced fluorescence change and an energy transduction pathway in S1 and by the significance of a basic understanding of a biochemically relevant tryptophan quenching mechanism (*52*). The importance of the relationship between ATP-induced absorption or fluorescence change and energy transduction has been appreciated for the many years since its discovery (*14*, *50*, *53*) and its consequences elegantly exploited by coupling myosin transient conformation with ATP hydrolysis (*33*, *54*). For now, how Trp510 is quenched will play a role in sorting out proposed molecular mechanisms for energy transduction. The intrinsic value of understanding a biochemically relevant tryptophan quenching mechanism will be measured in the broader implications of the present findings for understanding protein structure and dynamics.

Isolation of Trp510 emission, either by physical (differential spectroscopy) or biochemical (site-directed mutagenesis) means (*16*, *23*), is requisite to a definitive spectroscopic experiment elucidating the mechanism of Trp510 ATP sensitivity. Once accomplished, characterization of the Trp510 time-resolved fluorescence intensity decay amplitude and lifetime provide sufficient information to distinguish competing quenching schemes. We found that the primary quenching mechanism is static, meaning that Trp510 enters into a ground-state interaction with another local group from the S1 such that free (W) and interacting (W•Q) Trp510s have very different fluorescence characteristics (Scheme 2). W is fluorescent, but the W•Q complex does not detectably fluoresce because it rapidly decays to the ground state via nonradiative relaxation or because any fluorescence is far from the free tryptophan wavelength. The relative equilibrium concentrations of the W and W•Q forms are given by binding constant K_S. K_S depends on the occupant of the active site of S1. It is largest in the absence of nucleotide giving the lowest amplitude (because of static quenching) and longest relaxation time (because of delayed fluorescence) Trp510 fluorescence. K_S decreases distinctly for each nucleotide-bound conformation S1 assumes transiently during ATPase, giving increased amplitude and shorter relaxation time Trp510 fluorescence. The observed tryptophan absorption change upon nucleotide or nucleotide analogue binding is similarly tied to K_S because the static quencher also influences Trp510 absorption (*50*).

Time-resolved decay of Trp510 fluorescence was isolated by using site-directed mutagenesis of truncated DcS1 (*25*) and observed under conditions comparable to our experiments. There, Trp510 was shown to be statically quenched and to emit fluorescence with lifetimes of 1 and 5 ns. The amount of static quenching and the amplitude of the 5 ns fluorescence lifetime are modulated by nucleotide binding to cause Trp510's nucleotide sensitivity. Nucleotide binding does not affect the 1 ns lifetime component of Trp510 emission. These results are in accord with our findings regarding the contribution of static quenching to Trp510 nucleotide sensitivity. Concerning the number of lifetime components in the Trp510 fluorescence, our finding of a single long-lifetime relaxation in skeletal S1 appears to conflict with the findings from DcS1. However, the manner of isolating Trp510 fluorescence in skeletal S1 could be the source of the conflict. Fluoresceine in 5′F-S1 quenches Trp510 such that the difference in eq 2 contains only Trp510 fluorescence. If a short-lifetime component of Trp510 fluorescence relaxes too quickly to be efficiently quenched by the presence of the fluorescein probe, this component cancels when forming the difference in eq 2.

Potentially more fundamental differences emerge between the rabbit skeletal S1 and truncated DcS1 systems when comparing the effect of nucleotide binding on fluorescence relaxation time. In rabbit S1, decreased relaxation time accompanies nucleotide binding (due to less delayed fluorescence). In truncated DcS1, nucleotide binding causes an apparent relaxation time increase because the amplitude of the longer-lifetime component increases and the amplitude of the shorter-lifetime component remains unchanged. The latter observation is not inconsistent with Scheme 2 but indicates that delayed fluorescence does not contribute significantly to Trp510 emission in truncated DcS1. The contribution of delayed fluorescence is reduced by lowering $k_{W\text{•}\text{–}E}$ (exiplex dissociation) or by increasing k_E (exiplex decay rate) over that in skeletal S1.

With static quenching established as the basis for Trp510's nucleotide sensitivity, we looked to the S1 crystal structures to find the candidate quenchers. When it is noted that aromatic residues are the most capable of electric dipole−

dipole mediated interaction with Trp510, characteristic to the W•Q complex, and that the skeletal S1 crystal structure without nucleotide represents the open S1 conformation in which the W•Q complex has the highest probability for formation, Tyr503, Phe512, and Phe711 become the candidate static quenchers. In the open conformation of skeletal S1, these residues are 4−5 Å from Trp510. They all change their relationship with Trp510 significantly when S1 assumes the M** or M^ conformations from the smooth or scallop muscle crystal structures (Figure 2). Tyr503 and Phe512 remain at about the same distance, while Phe711 moves ∼2−4 Å away from Trp510 upon nucleotide binding. Computation of the Trp510 electronic wave function for the M, M**, and M^ S1 conformations shows a strong Tyr503−Trp510 electronic coupling in the M conformation that significantly diminishes upon formation of either the M^ or the M** conformations (Table 2). The substitution of Tyr503 with phenylalanine or leucine eliminates strong coupling between Trp510 and any other residue in S1 for all S1 conformations. Strong electronic coupling must exist between Trp510 and its static quencher, suggesting Tyr503 is the static quencher.

The absorption dipole strengths for the M, M^, and M** S1 conformations were computed from the Trp510 electronic wave function (Table 2). The strong Tyr503−Trp510 electronic coupling lowers the Trp510 dipole moment in the M conformation, an effect that is diminished upon nucleotide binding giving rise to the nucleotide sensitivity in Trp510 absorption. Replacement of Tyr503 with phenylalanine or leucine attenuates, but does not eliminate, nucleotide sensitivity in Trp510 absorption. Only the replacement of Tyr503 and Phe711 fully eliminates nucleotide sensitivity in Trp510 absorption. It appears that the 2−4 Å movement of Phe711 away from Trp510 upon nucleotide binding has a significant impact on nucleotide sensitivity in Trp510 absorption. Calculation also shows that Phe512, other aromatic groups, and the many peptide amide groups in the vicinity of Trp510 also perturb the Trp510 electronic wave function during the structural transitions implied by the crystal structures; however, their collective action largely cancels. The multiple peptide amide groups in the vicinity of Trp510, acting in concert, could readily reverse trends caused by Tyr503 and Phe711; however, this kind of spectroscopic cooperativity does not occur in the structures considered. On these bases, we propose Tyr503 as the static quencher of Trp510 giving rise to the latter's fluorescence sensitivity to nucleotide binding due to the changing Tyr503−Trp510 coordination during ATP hydrolysis. Nucleotide sensitivity in Trp510's absorption is a more delocalized phenomena because it dependens on both Tyr503−Trp510 and Phe711−Trp510 interactions.

In summary, competing mechanisms for Trp510 absorption and fluorescence sensitivity to nucleotide binding were distinguished on the basis of time-resolved fluorescence intensity measurements. The Trp510 fluorescence lifetimes and decay amplitudes indicated that its side chain forms a ground-state complex with a static quencher. The Trp510−quencher association constant depends on the S1 transient intermediate state occupied, thereby conferring nucleotide sensitivity to Trp510 fluorescence. Furthermore, this mechanism accounts, in part, for the observed nucleotide-induced optical density enhancement in Trp510 because the ground-state interaction also perturbs light absorption. Inspection of skeletal, smooth, and scallop muscle S1 crystal structures suggest candidates for the static quencher. The Trp510 electronic wave function, computed from these crystal structures, shows coupling to Tyr503 with a strength unmatched by any other group, suggesting Tyr503 is the static quencher of Trp510. The substitutions Tyr503Phe or Tyr503Leu suggest that Phe711 also contributes to nucleotide-induced optical density enhancement in Trp510.

ACKNOWLEDGMENT

We thank Drs. Katalin Ajtai and Stuart Taylor for assistance in completing this project.

REFERENCES

1. Maita, T., Yajima, E., Nagata, S., Miyanishi, T., Nakayama, S., and Matsuda, G. (1991) *J. Biochem. 110*, 75−87.
2. Morales, M. F., and Botts, J. (1979) *Proc. Natl. Acad. Sci. U.S.A. 76*, 3857−3859.
3. Toyoshima, Y. Y., Kron, S. J., McNally, E. M., Niebling, K. R., Toyoshima, C., and Spudich, J. A. (1987) *Nature 328*, 536−539.
4. Kitamura, K., Tokunaga, M., Iwane, A. H., and Yanagida, T. (1999) *Nature 397*, 129−134.
5. Rayment, I., Rypniewski, W. R., Schmidt-Base, K., Smith, R., Tomchick, D. R., Benning, M. M., Winkelmann, D. A., Wesenberg, G., and Holden, H. M. (1993) *Science 261*, 50−58.
6. Fisher, A. J., Smith, C. A., Thoden, J. B., Smith, R., Sutoh, K., Holden, H. M., and Rayment, I. (1995) *Biochemistry 34*, 8960−8972.
7. Gulick, A. M., Bauer, C. B., Thoden, J. B., and Rayment, I. (1997) *Biochemistry 36*, 11619−11628.
8. Smith, C. A., and Rayment, I. (1996) *Biochemistry 35*, 5404−5417.
9. Dominguez, R., Freyzon, Y., Trybus, K. M., and Cohen, C. (1998) *Cell 94*, 559−571.
10. Houdusse, A., Kalabokis, V. N., Himmel, D., Szent-Gyorgyi, A. G., and Cohen, C. (1999) *Cell 97*, 459−470.
11. Huxley, H. E. (1969) *Science 164*, 1356−1366.
12. Huxley, A. F., and Simmons, R. M. (1971) *Nature 233*, 533−538.
13. Spudich, J. A. (1994) *Nature 372*, 515−518.
14. Werber, M. M., Szent-Györgyi, A. G., and Fasman, G. D. (1972) *Biochemistry 11*, 2872−2883.
15. Marston, S. B., and Taylor, E. W. (1980) *J. Mol. Biol. 139*, 573−600.
16. Batra, R., and Manstein, D. J. (1999) *J. Biol. Chem. 380*, 1017−1023.
17. Yengo, C. M., Chrin, L. R., Rovner, A. S., and Berger, C. L. (2000) *J. Biol. Chem. 275*, 25481−25487.
18. Onishi, H., Konishi, K., Fujiwara, K., Hayakawa, K., Tanokura, M., Martinez, H. M., and Morales, M. F. (2000) *Proc. Natl. Acad. Sci. U.S.A. 97*, 11203−11208.
19. Bivin, D. B., Kubota, S., Pearlstein, R., and Morales, M. F. (1993) *Proc. Natl. Acad. Sci. U.S.A. 90*, 6791−6795.
20. Okamoto, Y., and Yount, R. G. (1985) *Proc. Natl. Acad. Sci. U.S.A. 82*, 1575−1579.
21. Papp, S., and Highsmith, S. (1993) *Biochim. Biophys. Acta 1202*, 169−172.
22. Park, S., Ajtai, K., and Burghardt, T. P. (1996) *Biochim. Biophys. Acta 1296*, 1−4.
23. Park, S., and Burghardt, T. P. (2000) *Biochemistry 39*, 11732−11741.
24. Birks, J. B. (1970) *Photophysics of Aromatic Molecules*, pp 403−491, Wiley-Interscience, New York.
25. Malnasi-Csizmadia, A., Kovacs, M., Woolley, R. J., Botchway, S. W., and Bagshaw, C. R. (2001) *J. Biol. Chem. 276*, 19483−19490.
26. Tonomura, Y., Appel, P., and Morales, M. (1966) *Biochemistry 5*, 515−521.

27. Weeds, A. G., and Taylor, R. S. (1975) *Nature 257*, 54−56.
28. Ajtai, K., and Burghardt, T. P. (1992) *Biochemistry 31*, 4275−4288.
29. Ajtai, K., Poto, L., and Burghardt, T. P. (1990) *Biochemistry 29*, 7733−7741.
30. Ajtai, K., Ilich, P. J. K., Ringler, A., Sedarous, S. S., Toft, D. J., and Burghardt, T. P. (1992) *Biochemistry 31*, 12431−12440.
31. Fiske, C. H., and Subbarow, Y. (1925) *J. Biol. Chem. 66*, 375−400.
32. Park, S., Ajtai, K., and Burghardt, T. P. (1999) *Biochim. Biophys. Acta 1430*, 127−140.
33. Trentham, D. R., Eccleston, J. F., and Bagshaw, C. R. (1976) *Q. Rev. Biophys. 9*, 217−281.
34. Taylor, R. S., and Weeds, A. G. (1976) *Biochem. J. 159*, 301−315.
35. Murhpy, C. T., Rock, R. S., and Spudich, J. A. (2001) *Nat. Cell Biol. 3*, 311−315.
36. Bagshaw, C. R., and Trentham, D. R. (1974) *Biochem. J. 141*, 331−349.
37. Goody, R. S., and Hofmann, W. (1980) *J. Muscle Res. Cell Motil. 1*, 101−115.
38. Peyser, Y. M., Ajtai, K., Burghardt, T. P., and Muhlrad, A. (2001) *Biophys. J. 81*, 1101−1114.
39. Werber, M. M., Peyser, Y. M., and Muhlrad, A. (1992) *Biochemistry 31*, 7190−7197.
40. Peyser, Y. M., Ajtai, K., Werber, M. M., Burghardt, T. P., and Muhlrad, A. (1997) *Biochemistry 36*, 5170−5178.
41. Maruta, S., Henry, G. D., Sykes, B. D., and Ikebe, M. (1993) *J. Biol. Chem. 268*, 7093−7100.
42. Geeves, M. A., and Holmes, K. C. (1999) *Annu. Rev. Biochem. 68*, 687−728.
43. Torgerson, P. M. (1984) *Biochemistry 23*, 3002−3007.
44. Badea, M. G., and Brand, L. (1979) *Methods Enzymol. 61*, 378−425.
45. Park, S., Ajtai, K., and Burghardt, T. P. (1996) *Biophys. Chem. 63*, 67−80.
46. Park, S., Ajtai, K., and Burghardt, T. P. (1997) *Biochemistry 36*, 3368−3372.
47. Lakowicz, J. R. (1983) *Principles of fluorescence spectroscopy*, pp 257−301, Plenum Press, New York.
48. Bayley, P. M., Nielsen, E. B., and Schellman, J. A. (1969) *J. Phys. Chem. 73*, 228−243.
49. Burghardt, T. P., Garamszegi, S. P., Park, S., and Ajtai, K. (1998) *Biochemistry 37*, 8035−8047.
50. Morita, F. (1967) *J. Biol. Chem. 242*, 4501−4506.
51. Valeur, B., and Weber, G. (1977) *Photochem. Photobiol. 25*, 441−444.
52. Chen, Y., and Barkley, M. D. (1998) *Biochemistry 37*, 9976−9982.
53. Cheung, H. C., and Morales, M. F. (1969) *Biochemistry 8*, 2177−2182.
54. Johnson, K. A., and Taylor, E. W. (1978) *Biochemistry 17*, 3432−3442.

BI0157058